

Measurement of ultrafast hot-carrier relaxation in silicon by thin-film-enhanced, time-resolved reflectivity

F. E. Doany and D. Grischkowsky

IBM Watson Research Center, Yorktown Heights, New York 10598

(Received 30 July 1987; accepted for publication 4 November 1987)

Time-resolved reflectivity measurements with ~ 100 fs resolution have revealed an initial 350 fs relaxation time in silicon, believed to be the time it takes hot, photoinjected carriers to relax to the band edge. The measurements were made at low carrier densities ($\sim 10^{17}$ cm $^{-3}$) for which carrier-carrier processes are negligible, and were facilitated by the greater than order of magnitude enhancement of the change in reflectivity signals that can be produced by the use of thin films.

Picosecond and femtosecond optical techniques have been extensively utilized in studies of the dynamics of non-equilibrium carrier relaxation in semiconductors.¹ When a semiconductor is excited with photons of energy $\hbar\omega$ greater than its band gap E_g , electron-hole pairs are created with excess kinetic energy $\hbar\omega - E_g$. This excess energy will then redistribute among the electronic and lattice degrees of freedom until equilibrium is reached with the surroundings. To date, most time-resolved reflectivity experiments in silicon have probed carrier relaxation after the thermalized distribution has been established. Numerous studies have examined the dynamics of dense electron-hole plasmas in silicon, particularly related to ultrafast heating and pulsed annealing.²⁻¹⁰ Shank *et al.*⁴ have recently used high intensity, 90 fs pulses to time resolve the transition to the melted state in silicon. In addition to the plasma reflectivity signal, the reflectivity dynamics near the melting threshold fluence exhibited an additional ~ 1 ps component. This fast component was believed to arise from lattice heating resulting from phonon emission due to hot-carrier relaxation toward the band edge. Lattice heating above the melting threshold leading to disorder in crystalline silicon was also probed by second-harmonic generation^{5,10} and the results are consistent with thermally induced disorder occurring within ~ 0.5 ps. Reflectivity changes monitored slightly below the melting threshold⁸ also suggest that direct heating of the lattice resulting from the hot-carrier relaxation occurs within 1 ps.

The above measurements are all indicative of a subpicosecond cooling time (energy relaxation time) for photoexcited carriers, although no direct experimental measurement is yet available. The carrier lifetime in amorphous silicon was measured as 0.8 ps by time-resolved reflectivity indicating the relaxation time is at least this fast.⁷ Hot-carrier relaxation times of approximately 0.5–1.0 ps in amorphous silicon have been estimated from photoinduced absorption measurements using laser pulse widths of ~ 0.8 ps.¹¹ Carrier lifetimes as short as 600 fs have been measured in ion-implanted Si suggesting that the cooling time is ≤ 600 fs.⁹ Steady-state measurements have also been used to obtain estimates of the energy relaxation times.¹² Analysis of the temperature dependence of these electron drift velocity measurements in silicon^{12,13} is consistent with energy relaxation times ranging from ~ 3 to ~ 0.4 ps for hot electrons (~ 300 – 500 K) in a 300-K silicon lattice. These rates have also been calculated by the Monte Carlo method^{12,14} as a function of

the difference between the average and the thermal energies. At a carrier density of 10^{17} cm $^{-3}$, this time varied from ~ 250 fs for carriers near the band gap to ~ 450 fs for carriers with 1 eV excess energy.

We report here results on the carrier relaxation dynamics in silicon obtained with high temporal resolution (~ 100 fs) and under low carrier densities ($\sim 10^{17}$ cm $^{-3}$) where carrier-carrier processes were negligible. The samples used in this study are 0.5- μ m-thick silicon films on sapphire (SOS) wafers. High signal-to-noise reflectivity measurements were obtained by taking advantage of the thin-film properties to enhance the observed changes in the reflectivity of silicon by more than an order of magnitude. This experimental technique is ideally suited for investigating the carrier dynamics in thin films of semiconductors.

Time-resolved reflectivity measurements were obtained using a system described elsewhere.⁹ Briefly, the laser source consists of a dispersion-compensated colliding-pulse mode-locked (cpm) ring dye laser producing 70 fs pulses at 2.0 eV (625 nm) and operating at a repetition rate of 100 MHz. A probe beam was split off the main pump beam and attenuated to about 2% of the ~ 1 mW pump power. The pump was incident onto the sample at an angle of $\sim 45^\circ$ to the surface normal and focused to a diameter of 10 μ m, while the probe was incident normal to the surface and focused to a diameter of 5 μ m. The polarization of the probe beam was rotated by 90° relative to the pump in order to suppress interferences between the two beams at the sample surface. Prior to reaching the sample, the probe beam was additionally split into two beams: one was reflected off the sample and detected on a large surface area photodiode, and the second was directed onto a matched photodetector and used as a reference. The signal and reference photocurrents were subtracted and the difference was detected using a lock-in amplifier referenced at the 2.7 kHz pump beam chopping frequency. This differential detection compensated for small fluctuations in the incident laser intensity and allowed for detection of changes in the probe beam reflectance of less than 1 part in 10^6 .

Using this apparatus, we have previously measured the time evolution of the reflectivity following photoexcitation of a SOS wafer on the ~ 100 ps timescale.⁹ The maximum change in reflectivity for the 1 mW pump power used in that study was $\Delta R/R \sim 3 \times 10^{-5}$. The observed change in reflectivity exhibited a pulse width limited rise time (< 150 fs) with a long time recovery of approximately 100 ps, consist-

tent with carrier diffusion out of the $10\ \mu\text{m}$ pump region with a drift velocity $10^7\ \text{cm/s}$.¹²

Both n - and p -type bulk silicon wafers exhibited similar time evolution as the SOS wafer. However, the maximum signals observed in these bulk samples at 1 mW pump power were only $\Delta R/R \sim 2 \times 10^{-6}$, less than 1/10 of that from SOS. The recovery of the reflectivity in these samples was slightly faster ($\sim 50\ \text{ps}$) than in SOS. This recovery is consistent with previous measurements⁴ and is due to carrier diffusion into the bulk. In SOS carriers are injected throughout the $0.5\ \mu\text{m}$ film and thus can only diffuse laterally out of the $10\ \mu\text{m}$ pump region. In the bulk wafers, however, diffusion into the bulk will dominate since the absorption depth is only $3\ \mu\text{m}$.¹⁵

The signal strength ($\Delta R/R$) observed in the bulk silicon is consistent with the index change associated with the plasma generated by the 1 mW pump power (10 pJ/pulse). Without pumping, the reflectivity at normal incidence of the bulk silicon wafers at 625 nm was 0.35. This same value can be calculated from the simple expression for the reflectance at normal incidence,

$$R_1 \equiv r_1^2 = [(n_1 - 1)/(n_1 + 1)]^2, \quad (1)$$

where the refractive index of silicon at 625 nm is $n_1 = 3.9$. In the Drude formalism the change in refractive index due to the presence of a low density electron-hole plasma is

$$\Delta n/n = -(2\pi e^2/\epsilon m \omega^2)N, \quad (2)$$

where ϵ is the background dielectric constant at low frequencies, m is the effective mass, and ω is the probe angular frequency. From Eq. (2), the calculated index change due to the plasma at our experimental conditions for which the injected carrier density $N \sim 2 \times 10^{17}\ \text{cm}^{-3}$ is $\Delta n_1 \sim 4 \times 10^{-6}$. This value, together with the change in reflectivity dR_1/dn_1 derived from Eq. (1), gives the predicted value $\Delta R_1/R_1 = 4 \times 10^{-6}$, in approximate agreement with the measurement $\Delta R_1/R_1 \sim 2 \times 10^{-6}$.

The above simple analysis does not apply to SOS, where the change in reflectivity was approximately an order of magnitude greater than that observed for bulk silicon under identical experimental conditions. Associated with this point is the fact that for SOS the reflectance was not constant across the wafer. At normal incidence, the reflectance varied from 0.18 to 0.55 for different positions on the surface of the 3-in. wafer indicating interferences arising from multiple reflections at the air/silicon and silicon/sapphire interfaces. The absorption, however, remained nearly constant at 0.3. For our $\sim 0.5\ \mu\text{m}$ film this corresponds to an absorption depth $\alpha^{-1} \sim 1.5\ \mu\text{m}$, consistent with earlier measurements on epi films.¹⁶

Figure 1(a) shows the calculated reflectance at normal incidence of a SOS film with thickness variation 0.45–0.55 μm . The solid curve was obtained from the thin-film equations¹⁷ including absorption ($\alpha^{-1} = 1.5\ \mu\text{m}$) but neglecting the small reflection at the sapphire/air interface. The reflectance varies from 0.15 to 0.55, depending on the film thickness l . For a simple but informative analysis we need only to consider two reflections. With an incident electric field E_0 , these first two reflections are $E_1 = r_1 E_0$ and $E_2 = T_1 r_2 E_0 e^{-\alpha l}$, where r_2 is the silicon/sapphire reflection co-

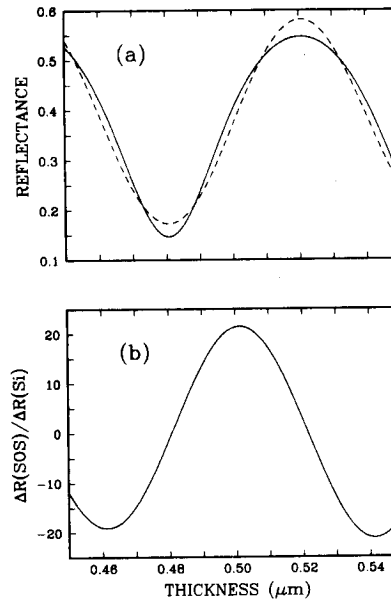


FIG. 1. (a) Calculated reflectance at 625 nm for a $0.5\text{-}\mu\text{m}$ film of silicon-on-sapphire (SOS) substrate. Solid line is from the full thin-film equations. Dashed line uses only the first two reflections. (b) Calculated change in reflectivity for SOS normalized to the change in reflectivity for a single Si surface $\Delta R(\text{SOS})/\Delta R(\text{Si}) = (dR/dn_1)/(dR_1/dn_1)$.

efficient $r_2 = (n_2 - n_1)/(n_2 + n_1)$, T_1 is the transmission of the silicon/air interface ($T_1 = 1 - R_1$), and n_2 is the refractive index of sapphire. The reflectance is then given by the time average of $[E_1(t) + E_2(t)]^2/E_0(t)^2$,

$$R = R_1 + 2(1 - R_1)r_1 r_2 e^{-\alpha l} \cos 2\phi + (1 - R_1)^2 R_2 e^{-2\alpha l}, \quad (3)$$

where $\phi = 2\pi n_1 l/\lambda$ is the phase delay introduced by propagation through the film; λ is the probe wavelength in air. This calculation (dashed line) is shown to be qualitatively similar to the full thin-film result (solid curve) in Fig. 1(a).

Calculating dR/dn_1 from Eq. (3), we obtain the change in reflectivity for SOS,

$$\frac{dR}{dn_1} = \frac{dR_1}{dn_1} + (F_1 \cos 2\phi + F_2 \sin 2\phi) e^{-\alpha l} + F_3 e^{-2\alpha l}. \quad (4)$$

The first term and third terms in this expression correspond to first and second surface reflections while the middle term arises from the interference between the two reflections. The functions F_1 and F_3 are independent of l , while F_2 varies linearly with l . Evaluating them for our conditions, we obtain $F_1 \sim 0.1$, $F_2 \sim -3.6l/\lambda$ (~ -3), and $F_3 \sim -0.06$. Because of the relatively large value of F_2 , the associated oscillating term dominates the changes in reflectivity since $dR_1/dn_1 \sim 0.1$. In Fig. 1(b) we show dR/dn_1 vs ϕ (sample thickness) normalized to the value for a single surface dR_1/dn_1 . Here one can see that for most thicknesses the magnitude of the thin-film interference term is far greater than the single surface term and peaks at a value of $20 \times$. Thus, in agreement with our observation, changes in reflectivity for SOS can be more than an order of magnitude greater than for bulk silicon.

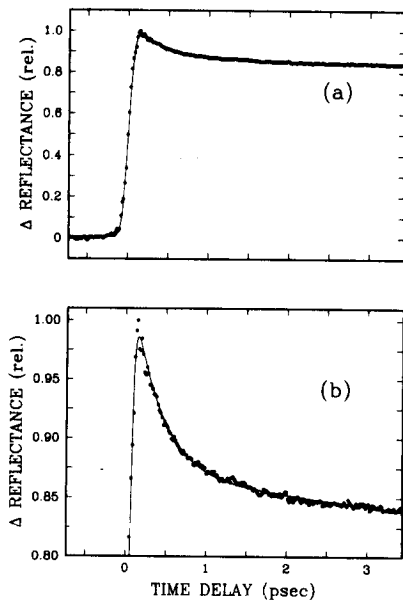


FIG. 2. (a) Transient reflectivity changes for SOS. (b) The top 15% of the data above on an expanded scale. The smooth curve in (a) and (b) is a biexponential fit with $\tau_1 = 350$ fs and $\tau_2 \sim 100$ ps.

Figure 2(a) shows the reflectivity signal for SOS during the first ~ 3 ps following photoinjection of carriers. In addition to the previously discussed ~ 100 ps component, the time evolution exhibits a fast component near $t = 0$. These data were modeled using a biexponential decay together with a 120-fs Gaussian experimental response function. By fixing the long time constant at 100 ps and using a least-squares fitting routine, the fast decay component was determined to be ~ 350 fs. This short time is clearly resolvable as evidenced by the < 150 fs rise time of the data in Fig. 2. The enhanced signal-to-noise levels of the data and the agreement of the model are evident from Fig. 2(b) which show in an expanded scale the top 15% of the data and the fit of Fig. 2(a). The power dependence of this decay time was also checked since relaxation rates may depend on carrier density at densities $> 10^{17} \text{ cm}^{-3}$.^{18,19} The carrier density for the experimental conditions used in obtaining the data in Fig. 2 is $\sim 2 \times 10^{17} \text{ cm}^{-3}$. Identical time evolution was observed when the laser power was reduced by a factor of 4.

The initial fast component is believed to be the hot-carrier cooling rate in silicon. The 2.0 eV excitation generates carriers with substantial excess kinetic energy since the band gap of silicon is only 1.15 eV at 293 K. Thus initially, the electron and hole share an excess energy of ~ 0.85 eV. The measured 350 fs decay in the reflectivity represents the cooling time of these hot carriers. The dependence of the energy relaxation time on the excess energy of the electrons in silicon at 293 K has been calculated by the Monte Carlo method.^{12,14} For a carrier density of 10^{17} cm^{-3} this time varied smoothly from ~ 450 fs at an excess energy of 1.0 eV down to ~ 250 fs near the band gap (excess energy < 0.02 eV).¹³ These values bracket our experimental result of 350 fs and are consistent with our interpretation.

The dependence of the reflectivity on the carrier temperature (excess energy) is not predicted by the simple Drude expression presented in Eq. (2). This expression, however, is only an approximation and does not include sev-

eral factors which may contribute to the observed dependence on carrier temperature. The effective mass m of the carriers is not a constant, as assumed in Eq. (2), but varies with the curvature (nonparabolicity) of the potential. Similarly, the dielectric background is commonly taken as the long wavelength limiting value ϵ_∞ , thus ignoring its energy dependence and response to the plasma resonances. Additionally, free-carrier absorption, which has a strong dependence on carrier excess energy,¹¹ will also contribute to the change in reflectivity. Further considerations show that the fast component should also contain a small contribution due to lattice heating. Equation (2) shows that the change in index due to the plasma is negative, $\Delta n < 0$. The change in index associated with heating, however, is positive, $\Delta n > 0$.^{6,8,15} Thus, a rise in lattice temperature results in a change in reflectivity in the opposite direction to the plasma signal. This direct lattice heating is derived from the emission of phonons by the hot carriers as they relax toward the band edge. The time constant associated with this process is therefore an upper limit to the carrier cooling time. Estimates of the magnitude of this component, however, suggest that direct lattice heating would be only a minor contribution to the observed reflectivity signal. For 2 eV excitation, the ratio of the change in index due to direct heating to that of the plasma has been estimated as ~ 0.1 for probe wavelength of $0.485 \mu\text{m}$ and < 0.01 for $1.0 \mu\text{m}$.⁸ In our experiment at a probe wavelength of $0.625 \mu\text{m}$, the measured ratio of the fast/slow component is ~ 0.25 , much too large to be explained by lattice heating.

We would like to acknowledge the many helpful discussions with J. Kash and the use of computer modeling routines developed by J. Misewich. This research was partially supported by the U.S. Office of Naval Research.

¹See, for example, *Ultrafast Phenomena V*, edited by G. R. Fleming and A. E. Siegman (Springer, New York, 1986).

²P. Liu, R. Yen, N. Bloembergen, and R. T. Hodgson, *Appl. Phys. Lett.* **34**, 864 (1979).

³D. von der Linde and N. Fabricius, *Appl. Phys. Lett.* **41**, 991 (1982).

⁴C. V. Shank, R. Yen, and C. Hirlimann, *Phys. Rev. Lett.* **50**, 454 (1983).

⁵C. V. Shank, R. Yen, and C. Hirlimann, *Phys. Rev. Lett.* **51**, 900 (1983).

⁶L. A. Lompre, J.-M. Liu, H. Kurz, and N. Bloembergen, in *Ultrafast Phenomena IV*, edited by D. H. Auston and K. B. Eisenthal (Springer, New York, 1984), p. 122.

⁷J. Kuhl, E. O. Gobel, Th. Pfeiffer, and A. Jonietz, *Appl. Phys. A* **34**, 105 (1984).

⁸M. C. Downer and C. V. Shank, *Phys. Rev. Lett.* **56**, 761 (1986).

⁹F. E. Doany, D. Grischkowsky, and C.-C. Chi, *Appl. Phys. Lett.* **50**, 460 (1987).

¹⁰H. W. K. Tom, G. D. Aumiller, and C. H. Brito-Cruz, in *XV International Quantum Electronics Conference Technical Digest Series 1987* (Optical Society of America, Washington, D. C., 1987), Vol. 21, p. 26.

¹¹Z. Vardenay and J. Tauc, *Phys. Rev. Lett.* **18**, 1223 (1981).

¹²G. Canali, C. Jacoboni, F. Nava, G. Ottaviani, and A. Alberigi-Quaranta, *Phys. Rev. B* **12**, 2265 (1975).

¹³B. R. Nag, in *Semiconductors Probed by Ultrafast Laser Spectroscopy*, edited by R. R. Alfano (Academic, New York, 1984), Vol. I, p. 3.

¹⁴E. Constant, in *Hot Electron Transport in Semiconductors*, edited by L. Reggiani (Springer, New York, 1985), p. 227.

¹⁵G. E. Jellison, Jr. and F. A. Modine, *J. Appl. Phys.* **53**, 3745 (1982).

¹⁶R. Hulthen, *Phys. Scr.* **12**, 342 (1975).

¹⁷O. S. Heavens, *Thin Film Physics* (Methuen & Co., London, 1970).

¹⁸J. A. Kash and J. C. Tsang, in *Ultrafast Phenomena V*, edited by G. R. Fleming and A. E. Siegman (Springer, New York, 1986), p. 188.

¹⁹W. Z. Lin, J. G. Fujimoto, E. I. Ippen, and R. A. Logan, *Appl. Phys. Lett.* **50**, 124 (1987).